Colloids and Surfaces A: Physicochem. Eng. Aspects 497 (2016) 63–71

Contents lists available at ScienceDirect

Colloids and Surfaces A: Physicochemical and Engineering Aspects

journal homepage: www.elsevier.com/locate/colsurfa

Adsorption of phenol, phosphate and Cd(II) by inorganic–organic montmorillonites: A comparative study of single and multiple solute

Lingya Ma[a,b,c], Jianxi Zhu[a,d], Yunfei Xi[b,e,*], Runliang Zhu[a,d], Hongping He[a,d,**], Xiaoliang Liang[a,d], Godwin A. Ayoko[b]

[a] CAS Key Laboratory of Mineralogy and Metallogeny, Guangzhou Institute of Geochemistry, Chinese Academy of Sciences, Guangzhou 510640, China
[b] School of Chemistry, Physics and Mechanical, Science and Engineering Faculty, Queensland University of Technology (QUT), 2 George Street, GPO Box 2434, Brisbane, QLD 4000, Australia
[c] University of Chinese Academy of Sciences, Beijing 100049, China
[d] Guangdong Provincial Key Laboratory of Mineral Physics and Material, Guangzhou 510640, China
[e] Institute for Future Environments, Queensland University of Technology (QUT), Brisbane, QLD 4000, Australia

HIGHLIGHTS

- IOMt could simultaneously remove phenol, phosphate and Cd.
- The adsorption of phenol was not affected by phosphate and Cd and vice versa.
- The removal of phosphate and Cd were enhanced by synergistically adsorptions.
- The types of surfactant affected adsorption capacities of IOMts.

GRAPHICAL ABSTRACT

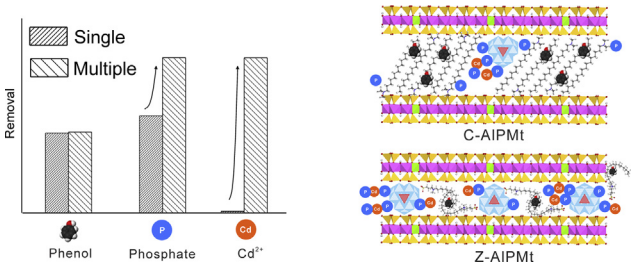

ARTICLE INFO

Article history:
Received 16 November 2015
Received in revised form 17 February 2016
Accepted 24 February 2016
Available online 26 February 2016

Keywords:
Inorganic-organic montmorillonite
Adsorption
Phenol
Cadmium
Phosphate

ABSTRACT

Inorganic-organic montmorillonites (IOMts) obtained by modifying polyhydroxy-aluminum (Al_{13})-pillared montmorillonite (AlPMt) with the cationic surfactant (C16) and zwtterionic surfactant (Z16) were investigated with the aim to remove phenol, phosphate and Cd(II) simultaneously. The structures of IOMts prepared using different surfactant doses (0.4 and 1.0CEC) strongly depended on the types and doses of the surfactants. The Al_{13} contents of C16 modified AlPMts (C-AlPMts) decreased with increasing C16 loading while that of Z16 modified AlPMt (Z-AlPMts) did not. In the single adsorption system, all IOMts could efficiently remove phenol and phosphate, but not Cd(II). IOMts, however, could efficiently remove all three contaminants simultaneously in the multi-contaminant adsorption system. The adsorptions of phenol on IOMts were not affected by the other two inorganic components and vice versa. Whereas the adsorptions of phosphate and Cd(II) were significantly enhanced in the multi-contaminant system, and the adsorption of one increased with increasing initial concentration of the other one, especially the adsorption of Cd(II). The enhancements of adsorption of phosphate and Cd(II) on the IOMts with higher Al_{13} content were much larger than that on IOMts with lower Al_{13} content. The adsorption mechanism for phosphate and Cd(II) uptake in the multi-contaminant system possible involve the formation of phosphate-bridged ternary complexes.

* Corresponding author at: School of Chemistry, Physics and Mechanical, Science and Engineering Faculty, Queensland University of Technology (QUT), 2 George Street, GPO Box 2434, Brisbane, QLD 4000, Australia.
** Corresponding author at: CAS Key Laboratory of Mineralogy and Metallogeny, Guangzhou Institute of Geochemistry, Chinese Academy of Sciences, Guangzhou 510640, China.
E-mail addresses: y.xi@qut.edu.au (Y. Xi), hehp@gig.ac.cn (H. He).

http://dx.doi.org/10.1016/j.colsurfa.2016.02.032
0927-7757/

1. Introduction

Because of industrial and agricultural activities, toxic chemicals are released and transported into water and soils. This does not only result in degradation of environmental quality but also become a potential threat to animal and human health *via* the food chain [1,2]. Organic contaminants, heavy metals, and oxyanions are the typical contaminants in environment. Many organic contaminants (*e.g.* aromatic compounds) and heavy metals (*e.g.* cadmium) are potential carcinogens and/or mutagens [1]. Although phosphate, a common type of oxyanion, is an essential nutrient for plants, high concentration of phosphate causes risks to the environment, such as the eutrophication of lakes and rivers [3]. Adsorption is considered to be one of the most common processes for the removal of these pollutants from water and many types of adsorbents have been developed accordingly. For example, activated carbons and porous materials are used to adsorb organic contaminants, heavy metals, or phosphates [4–6]. However, few adsorbents are available to simultaneously remove all of these contaminants in one step. As cost effective, efficient and sustainable adsorption materials, naturally occurring clay minerals have been recognized as practical and versatile template materials to treat a wide range of contaminants [7,8]. In this context, montmorillonite is a typical example of an abundant clay mineral that has been widely used in environmental remediation.

Organo-montmorillonite (OMt), modified by surfactant, is proved to be an efficient adsorbent for organic contaminants [8–10]. Hydroxyl-metal pillared montmorillonites, on the other hand, exhibits a strong affinity for heavy metals and phosphate [11–16]. Inorganic-organic montmorillonite (IOMts), intercalated by both surfactant and hydroxyl-metal, have been developed to remove both organic and inorganic contaminants [17–19]. The adsorption capacities of IOMts toward organic contaminants and phosphate or organic contaminants and heavy metal cations have received a lot of attention [20–23]. Little attention, however, has been paid to the simultaneous adsorption of all three contaminants on IOMts. In the environment, organic contaminant, phosphate and heavy metal cations often coexist in soil and wastewater, thus their transport and fate may be significantly influenced by mutual effects among them. Therefore, the adsorption behavior of organic contaminants, phosphate, and heavy metal cations on IOMts is worth studying. The findings may provide novel information for developing new effective IOMt adsorbents toward multi-contaminant, which are often encountered in practical scenarios.

The conventional IOMt is prepared by cationic surfactants, *e.g.* quaternary ammounium [8–10]. Previous studies showed that the type of organic modifier used could remarkably influence the structure and adsorptive behavior of OMt [24,25]. Sulfobetaine containing both positively charged (quaternary ammonium) and negatively charged (sulfonate) groups is a type of zwitterionic surfactant. Besides being highly water-soluble, biodegradable and biologically safe, sulfobetaine can retain its zwitterionic character over a broad pH range [25]. It might therefore be expected that the IOMt, intercalated with zwitterionic surfactant and hydroxyl-metal, will have novel properties and adsorption capacities toward a wide range of contaminants.

To better understand how to functionalize IOMt for environmental applications, comparative experimental work between cationic and zwitterionic surfactant prepared IOMts is still needed. Hence, in this study, IOMts were obtained by modifying Al_{13}-pillared montmorillonite (AlPMt) with a cationic surfactant (C16) and a zwitterionic surfactant (Z16), denoted as C-AlPMts and Z-AlPMts, respectively (Fig. 1). Al_{13} denotes the polyhydroxy-aluminum (Keggin) cation ($[Al^{IV}Al^{VI}{}_{12}O_4(OH)_{24}(H_2O)_{12}]^{7+}$). The structures and adsorption properties of the resulting IOMts were investigated. As common contaminants in the environment, phenol, Cd(II), and phosphate were selected as examples of organic contaminants, heavy metal cations and oxyanions, respectively. Both single contaminant and multi-contaminant adsorptions onto IOMts were studied for comparison. Authors reasoned that the results of this work could provide novel information for preparation and possible application of IOMts in simultaneous removal of organic contaminants, heavy metal cations and oxyanions from wastewater.

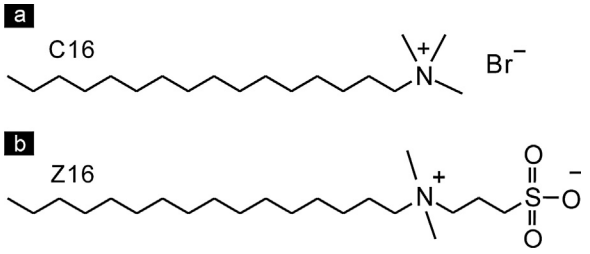

Fig. 1. Chemical structure of the surfactants: (a) cationic surfactant, hexadecyltrimethylammonium bromide, denoted as C16; and (b) zwitterionic surfactant, hexadecyldimethyl(3-sulphonatopropyl) ammonium, denoted as Z16.

2. Materials and methods

2.1. Materials

The calcium-rich montmorillonite (Ca-Mt; purity >95%) was obtained from Inner Mongolia, China. The cation exchange capacity (CEC) is 110.5 meq/100 g. The C16 and Z16 surfactants (Fig. 1), with purities 99%, were purchased from Nanjing Robiot Co., Ltd. Phenol was purchased from Shanghai RichJoint Chemical Reagents Co., Ltd. while $Cd(NO_3)_2$ and KH_2PO_4 were purchased from Guangzhou Chemical Reagent Factory. All chemicals were of analytical grades and used without further purification.

2.2. Preparation of IOMts

The preparation of IOMt was similar to the method of Ma et al. (2014). A hydroxyl-aluminum solution, containing Al_{13} cations, was obtained by slowly adding a 0.5 M Na_2CO_3 solution to a 1.0 M solution of $AlCl_3$ at a rate of 1 mL/min with vigorous stirring in a water bath at 60 °C to give a final OH^-/Al^{3+} ratio of 2.4. The mixture was continuously stirred for 12 h, after which it was allowed to 'age' for 24 h at 60 °C. 20 g montmorillonite was then added to the mixture to give an Al/clay ratio of 10 mmol/g. The dispersion was stirred for 24 h, and then aged for 24 h at 60 °C. The product was collected by centrifugation, washed 8 times with distilled water, and then freeze-dried for 48 h. The Al_{13}-pillared montmorillonite was denoted as AlPMt.

IOMts were obtained by dissolving a certain amount of surfactant in distilled water under stirring at 60 °C for 0.5 h, and then adding above fresh (nonfreeze-dried) AlPMt. The products were collected by centrifugation after stirring for 12 h at 60 °C, and washed 8 times with distilled water, then freeze-dried for 48 h. The amount of surfactants added was equivalent to 0.4 and 1.0 times the CEC of montmorillonite. The products prepared from AlPMt by adding 0.4CEC of C16 and Z16 surfactants were denoted as $C_{0.4}$-AlPMt and $Z_{0.4}$-AlPMt, respectively. Similarly, the other IOMt samples were marked by subscripts indicating the CEC multiplier.

2.3. Characterization of adsorbents

Powder X-ray diffraction (XRD) patterns were recorded on a Bruker D8 Advance diffractometer with Ni-filtered CuKα radiation (λ = 0.154 nm, 40 kV and 40 mA) between 1° and 20° (2θ) at a

scanning speed of 1° (2θ) min^{-1} with a 0.01 2θ step size and a 0.65 s counting time.

Nitrogen adsorption-desorption isotherms were determined on a Micromeritics ASAP 2020 M instrument. Samples were outgassed under vacuum for 12 h at 120 °C before determination. The multiple-point Brunauer-Emmett-Teller (BET) method was used to calculate the specific surface area of the materials.

The C, H, and N elemental microanalyses were performed in an Elementar Vario EL III Universal CHNOS Elemental Analyzer. Major elemental analysis was conducted on a Rigaku RIX 2000 X-ray fluorescence (XRF) spectrometer.

2.4. Adsorption experiments

The adsorption experiments were undertaken using two systems: (1) adsorption of a single contaminant; (2) simultaneous adsorption of three contaminants. For the first system (#1), the adsorption of phenol, phosphate or Cd(II) on samples was measured with an initial concentration of 25–175 mg/L for phenol, 20–140 mg/L for phosphate, and 30–210 mg/L for Cd(II). For the second (#2), three components were adsorbed simultaneously on the samples. The initial concentration of one contaminant was varied similarly to that in system #1, the other two were kept constants at 200 mg/L for phenol, 80 mg/L for phosphate or 90 mg/L for Cd(II).

Batch experiments were performed to study the adsorption capacities of IOMts from aqueous solutions. The initial pH was adjusted to ~5.0 (±0.05) using HCl and KOH. In a typical experiment in both systems, 0.1 g of the prepared adsorbent was combined with 20 mL solution containing different concentrations of phenol, phosphate and Cd(II) in a 25 mL glass centrifuge tube with Teflon cover. The tube was continuously agitated on a shaker for 24 h (Preliminary experiments indicated that the adsorption equilibrium of all three contaminants on IOMts could be reached within 4 h) at 160 rpm and 25 °C, and then filtered. The concentration of phenol in the supernatant was measured on UV–vis spectrophotometer (Perkin Elmer LAMBDA 850) at a wavelength of 270 nm; that of phosphate was analyzed using the Ascorbic Acid method [26] on a UV–vis spectrophotometer (Perkin Elmer LAMBDA 850) at a wavelength of 880 nm, and that of Cd(II) was determined by atomic absorption spectrometry (Perkin Elmer AAnalyst 400). The concentration of Br^- in the supernatant after the adsorption of phosphate onto C-AlPMt was measured by ion chromatography (Dionex ICS-900). Control experiments indicated no loss of any of the three contaminants in solution in the adsorption process with no interference occurring among the three contaminants during their analysis. All the adsorption experiments were, at least, conducted in duplicate.

3. Results and discussion

3.1. Structure of adsorbents

The basal spacing of original Ca-Mt was of 1.49 nm (Fig. 2), indicating a typical 001 plane of calcium montmorillonite. The d_{001}-value of 1.88 nm for the AlPMt corresponded to an interlayer space of 0.92 nm (Fig. 2). This value was close to the dimension of Keggin-like Al_{13} cation (0.9 nm), indicating the successful intercalation of Al_{13} into Ca-Mt [27]. After modification by C16, the d_{001}-value of 1.79 nm for C0.4-AlPMt was slightly smaller than that of AlPMt. When the amount of added C16 was increased to 1.0CEC, however, the d_{001}-value expanded to 2.07 nm, which suggested that the interlayer space of AlPMt could be further expanded by the intercalated C16. On the other hand, the d_{001}-values of Z16-modified AlPMt (~1.90 nm) were compareable with the d_{001}-value of the parent AlPMt (1.88 nm) regardless of whether the dose of the surfactant was 0.4 or 1.0CEC (Fig. 2). This observation indicated that Z16 either failed to penetrate the interlayer of AlPMt, or was loaded in the interlayer space of AlPMt in a configuration that caused no interlayer expansion [28].

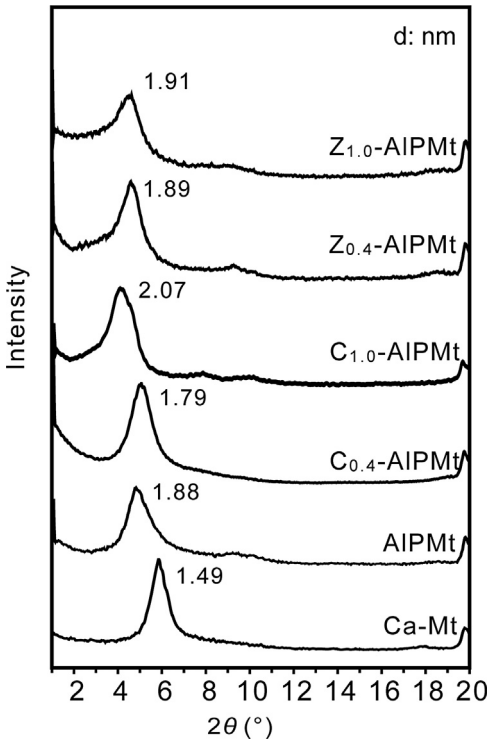

Fig. 2. X-ray diffraction patterns of raw montmorillonite (Ca-Mt), Al_{13}-pillared montmorillonite (AlPMt) and its interlayer complexes with the cationic surfactant C16 (C-AlPMt) and the zwitterionic surfactant, Z16 (Z-AlPMt) at different surfactant doses.

Table 1
Structural characteristic of original and C16- and Z16-modified Al_{13}-pillared montmorillonites.

Samples	d_{001} value (nm)	f_{oc} (%)	Al/Si[a]	CaO (%)	Specific surface areas (m^2/g)
Ca-Mt	1.49	0.04	0.29	2.29	65.6
AlPMt	1.88	0.05	0.49	Trace	283.2
$C_{0.4}$-AlPMt	1.79	8.27	0.41	Trace	20.7
$C_{1.0}$-AlPMt	2.07	17.94	0.37	Trace	10.1
$Z_{0.4}$-AlPMt	1.89	8.15	0.50	Trace	24.3
$Z_{1.0}$-AlPMt	1.90	11.68	0.49	Trace	18.5

Trace: The contents were lower than the detection limit of CaO (0.007%).
[a] Al/Si is the mass ratio of Al to Si.

The percentages of organic carbon (f_{oc}, wt.%), determined by elemental analysis, were used to estimate the amount of loaded surfactant (Table. 1). When the dose of surfactant was 0.4CEC, the f_{oc} value of $C_{0.4}$-AlPMt (8.27%) was comparable to that of $Z_{0.4}$-AlPMt (8.15%). The f_{oc} value of $C_{1.0}$-AlPMt (17.94%), however, was much larger than that of $Z_{1.0}$-AlPMt (11.68%). This finding suggests that Z16 successfully loaded on the AlPMt but the loaded amount was less than C16 when the dose of surfactant increased to 1.0CEC.

Variations in the Al content of the samples were deduced from the changes in the Al/Si ratio since the modification would not affect the amount of silicon in the montmorillonite structure (Table 1). After intercalation of Al_{13} cation, the Al/Si ratio increased from 0.29 for Ca-Mt to 0.49 for AlPMt, and the calcium content was lower than the detention limit, indicating the successful intercalation of Al_{13} *via* cation exchange with original calcium ions. With increased loaded amount of C16, however, the Al/Si ratio of C-AlPMt markedly decreased from 0.41 for $C_{0.4}$-AlPMt to 0.37 for C1.0-AlPMt,

Table 2
Linear regression data for the adsorption isotherms of phenol by IOMts in single and multi-contaminant adsorption systems.

	Linear equation	R^2	K_d (L/kg)	K_{oc} (L/kg)
$C_{0.4}$-AlPMt	$Q_e = 0.042C_e$	0.993	42	507.86
$C_{1.0}$-AlPMt	$Q_e = 0.131C_e$	0.998	131	730.21
$Z_{0.4}$-AlPMt	$Q_e = 0.036C_e$	0.996	36	441.72
$Z_{1.0}$-AlPMt	$Q_e = 0.054C_e$	0.991	54	462.32
$C_{0.4}$-AlPMt/m*	$Q_e = 0.040C_e$	0.990	40	483.68
$C_{1.0}$-AlPMt/m	$Q_e = 0.136C_e$	0.992	136	758.08
$Z_{0.4}$-AlPMt/m	$Q_e = 0.038C_e$	0.998	38	466.26
$Z_{1.0}$-AlPMt/m	$Q_e = 0.052C_e$	0.987	52	445.21

* The adsorption isotherms of phenol on C-AlPMts and Z-AlPMts in the multi-contaminant adsorption system ($C_{0,P}$ = 80 mg/L and $C_{0,Cd}$ = 90 mg/L) were denoted as C_n-AlPMt/m and Z_n-AlPMt/m, respectively. (n = the dose of surfactant).

indicating that partial replacement of Al_{13} cations in the interlayer space of AlPMt by C16 cations [19]. In the case of Z-AlPMt, the Al/Si ratio of Z-AlPMt was closely similar to that of the parent AlPMt (Table 1), suggesting that the modification of Z16 had little, if any, effect on the Al content of Z-AlPMts.

The specific surface area of AlPMt (283.2 m^2/g) was much larger than that of Ca-Mt (65.6 m^2/g) (Table 1), which was attributed to the expansion of montmorillonite's interlayer space by Al_{13} cations [17]. After modification of surfactant, the specific surface areas of both C-AlPMts and Z-AlPMts dramatically decreased since the interlayer space were blocked by loaded surfactant (Table 1).

The above characterization results indicated that the structure of IOMts strongly depended on the types and doses of the surfactants. For C-AlPMt, C16 could load on AlPMt by cation exchange with pre-intercalated Al_{13} cations. As a result, the basal spacing and f_{oc} of C-AlPMt increased with increasing C16 dose, but the loaded amount of Al_{13} cation decreased. In the case of Z-AlPMt, The Al_{13} cations cannot be replaced during the modification of Z16 and this prevents interlayer expansion. As a result, the maximum loading of Z16 was less than that of C16 on AlPMt. Z16 might occupy the pore space between the interlayer Al_{13} pillars [19,28], and/or the external surface of AlPMt.Because of the evident difference in the structure of IOMts with different surfactants, their adsorption capacities towards the three contaminants could be quite different.

3.2. Single contaminant adsorption

According to the adsorption isotherms of phenol on IOMts, the adsorption capacities of IOMts toward phenol decreased with decrease in f_{oc}, in the order: $C_{1.0}$-AlPMt > $Z_{1.0}$-AlPMt > $C_{0.4}$-AlPMt > $Z_{0.4}$-AlPMt (Fig. 3a). The adsorption isotherms of phenol were fitted by linear equation (Eq. (1)).

$$Q_e = K_d C_e \quad (1)$$

where the Q_e and C_e are the amount of solute adsorbed by adsorbent at equilibrium, K_d is the adsorption coefficient. The R^2 values showed that the linear equation is good fit for adsorption isotherm data (Table 2). The adsorption coefficient K_d, which was determined by the ratio of adsorbent bound solutes to mobile portion in solution [21], was often used to characterize the adsorption capacity of surfactant-modified minerals toward organic compounds. The calculated K_d value of $Z_{1.0}$-AlPMt was slightly larger than that of $C_{0.4}$-AlPMt and $Z_{0.4}$-AlPMt, but much smaller than that of $C_{1.0}$-AlPMt (Table 2).

Phenol is weakly acidic and its p*K*a is 9.95 in aqueous solution. The initial pH of adsorption test in present study was 5 and the values of equilibrium pH were below 6. Therefore, phenol molecules almost existed as non-ionic organic compounds (NOCs) in the pH range used for the adsorption tests. The adsorption of NOCs on surfactant-modified adsorbents has been considered as a partition process that is the NOCs are partitioned into the surfactant

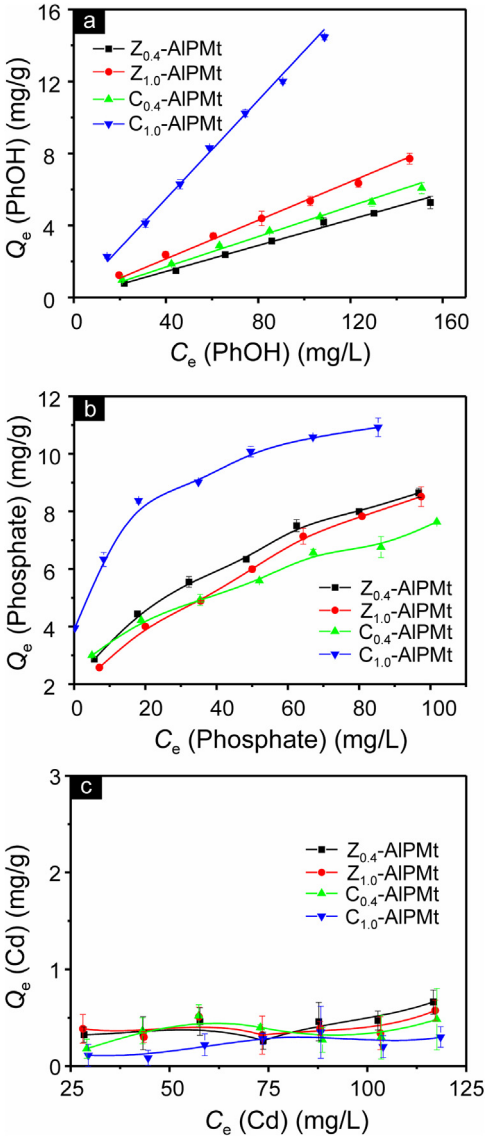

Fig. 3. Adsorption isotherms of phenol (a), phosphate (b), and Cd(II) (c) on IOMts in the single adsorption system.

alkyl chain formed organic phases [21]. Therefore, the organic carbon contents normalized adsorption coefficient ($K_{oc} = K_d/f_{oc}$) has been suggested to be a more appropriate parameter for evaluating the adsorption efficiency of surfactant modified adsorbents [21]. The K_{oc} value of $Z_{0.4}$-AlPMt was comparable with that of $Z_{1.0}$-AlPMt (Table 2), indicating they had similar adsorption capacities toward phenol. The K_{oc} value of $C_{0.4}$-AlPMt was slightly larger than that of Z-AlPMt (Table 2). $C_{1.0}$-AlPMt, however, had the largest K_{oc} value compared with other adsorbents, which implied that the C16 formed a more effective organic phase toward phenol on $C_{1.0}$-AlPMt.

In previous studies, the adsorption of phosphate on hydroxylmetal-montmorillonite was mainly controlled by ligand exchange between phosphate and hydroxyl group of hydroxylmetal [13,14,21,29,30]. Thus, the adsorption capacity of AlPMt strongly depended on the amount of loaded Al_{13} cations. Moreover, the exchangeable counter anions (Br^-) on C-AlPMt also could contribute to the adsorption of oxyanions [31,32], since cationic surfactant could intercalate in AlPMt as molecules (ion pairs) *via* van de Waals force between alkyl chains [18,19].

Table 3
Langmuir and Freundlich equation parameters for the adsorption of phosphate (P) on IOMts in single and multi-contaminant adsorption systems.

	Langmuir model			Freundlich model		
	Q_m (mg/g)	K_L (L/mg)	R^2	K_F	n	R^2
$C_{0.4}$-AlPMt	8.40	0.055	0.966	1.84	3.44	0.990
$C_{1.0}$-AlPMt	11.89	0.118	0.992	5.05	5.77	0.998
$Z_{0.4}$-AlPMt	10.31	0.044	0.976	1.44	2.56	0.997
$Z_{1.0}$-AlPMt	10.98	0.029	0.952	1.01	2.17	0.992
$C_{0.4}$-AlPMt/m*	10.07	0.158	0.986	3.89	4.85	0.992
$C_{1.0}$-AlPMt/m	12.13	0.181	0.990	5.47	6.11	0.998
$Z_{0.4}$-AlPMt/m	13.04	0.185	0.988	4.93	4.70	0.997
$Z_{1.0}$-AlPMt/m	12.36	0.183	0.990	4.42	4.36	0.997

* The adsorption isotherms of phosphate on C-AlPMts and Z-AlPMts in the multi-contaminant adsorption system ($C_{0,Phenol}$ = 200 mg/L and $C_{0,Cd}$ = 90 mg/L) were denoted as C_n-AlPMt/m and Z_n-AlPMt/m, respectively. (n = the dose of surfactant).

Adsorption isotherms of phosphate on IOMts were compared in Fig. 3b. In order to better understand the adsorption of phosphate on IOMts, Langmuir (Eq. (2)) and Freundlich isotherm (Eq. (3)) models were used to quantitatively descript the adsorption isotherm of phosphate (Table 3).

$$\frac{C_e}{Q_e} = \frac{1}{K_L Q_m} + \frac{C_e}{Q_m} \quad (2)$$

$$\lg Q_e = \lg K_F + \frac{1}{n}\lg Q_e \quad (3)$$

where Q_m is the maximum adsorption capacity, K_L is the Langmuir constant, and K_F and n are the constants of the Freundlich adsorption isotherm. As indicated by the R^2 values (Table 3), the Freundlich model presented a better fit for phosphate adsorption data than the Langmuir model in single adsorption system. The Freundlich model is applicable to multilayer adsorption on heterogeneous surface [33]. The observer better fit of the experimental data with freundlich isotherm can attribute to heterogeneous distribution of active sites on IOMts [33,34].

The adsorption capacities of IOMts toward phosphate increased in the order: $C_{0.4}$-AlPMt < $Z_{1.0}$-AlPMt ≈ $Z_{0.4}$-AlPMt < $C_{1.0}$-AlPMt (Fig. 3b). The adsorption capacities of IOMts had no evident correlation with their specific surface area values and Al contents at all. For Z-AlPMts, the adsorptions of phosphate were mainly contributed by the ligand exchange mechanism. The adsorption capacity of $Z_{0.4}$-AlPMt was slight higher than that of $Z_{1.0}$-AlPMt because more intercalated Z16 might occupy more adsorption sites of phosphate on $Z_{1.0}$-AlPMt than that on $Z_{0.4}$-AlPMt. Although Al contents of C-AlPMt were much less than those of Z-AlPMts, their adsorption capacities toward phosphate were comparable with ($C_{0.4}$-AlPMt) or much higher ($C_{1.0}$-AlPMt) than those of Z-AlPMts. Evident releases of Br ions from C-AlPMts were accompanied with the adsorption of phosphate on C-AlPMts (Fig. 4). The amount of released Br ions from $C_{1.0}$-AlPMt increased with increasing amount of adsorbed phosphate, but the amount of released Br ions from $C_{0.4}$-AlPMt was almost constant with increase in the adsorbed phosphate (Fig. 4). This finding suggests the adsorptions of phosphate on C-AlPMts were corresponded to both ligand exchange with hydroxyl group and anion exchange with Br^-, and the high adsorption of phosphate on $C_{1.0}$-AlPMt was primarily attributed by the large amount of Br^- ions on intercalated C16.

The adsorptions of Cd(II) on IOMts were extremely low in the single contaminant adsorption system (Fig. 3c). Montmorillonite is able to efficiently adsorb heavy metal cations from water through cation exchange [35]. The intercalation of Al_{13} cations and surfactant, however, resulted in the dramatic decrease of the adsorption capacities toward Cd(II), since both surfactants and high charged Al_{13} (7 +) cations are not readily exchangeable in the interlayer space of IOMts. Binding with Al_{13} cations in the interlayer space, the negatively charged groups of Z16 were not of benefit to the adsorption of Cd(II) on Z-AlPMt.

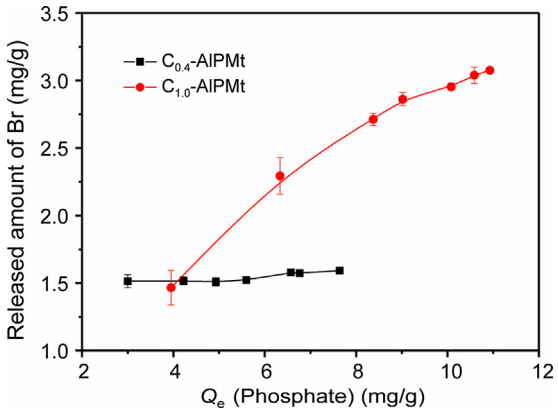

Fig. 4. Released amount of Br^- from C-AlPMts with the adsorption of phosphate in the single adsorption system.

3.3. Multiple contaminant adsorptions

3.3.1. Adsorption of phenol in the multi-contaminant system

According to comparative adsorption (Fig. 5a) and adsorption isotherms of phenol (Fig. 6a), the adsorption capacities of all IOMts in the multi-contaminant adsorption system were comparable to that in the single adsorption system. The K_d and K_{oc} values of all IOMts were also similar to that in the single adsorption systems (Table. 2). The adsorptions of phenol on IOMts were not influenced by increasing the initial concentration of phosphate (Fig. 6b), and neither did that by Cd(II) (Fig. 6c). These findings indicated that the adsorptions of phenol on IOMts were not affected by phosphate and Cd(II), which may be due to the different adsorption sites for phenol and other two inorganic contaminants. Phenol partitioned into the organic phase of the interlayer space, which was formed by alkyl chains of the surfactants. Whereas, the adsorptions of Phosphate and Cd(II) were mainly determined by the intercalated Al_{13} cations and hydrophilic groups of surfactant on IOMts.

3.3.2. Adsorption of phosphate and Cd(II) in the multi-contaminant system

Different from the adsorption of phenol, the adsorptions of phosphate and Cd(II) on IOMts were significantly enhanced in the multi-contaminant system (Fig. 5b,c). The adsorptions of both phosphate and Cd(II) were not affected by increasing of phenol concentration (Fig. 7b, 8b), this is attributed to the different adsorption sites of phenol and other two inorganic contaminants. Thus, the adsorption of phosphate and Cd(II) in the multi-contaminant system might be enhanced by synergistically adsorptions between phosphate and Cd(II).

According to the equilibrium adsorption studies in multi-contaminant system, the Langmuir adsorption capacities of IOMts toward phosphate are higher than that in single system (Table 3). Similar with the adsorption in single system, Freundlich model describe phosphate adsorption on IOMts better than Langmuir model (Table 3), suggesting the multilayer adsorption of phosphate on IOMts in multi-contaminant system. With the increase in Cd(II) concentration, the adsorptions of phosphate on IOMts were evidently enhanced (Fig. 7c), especially for the adsorption on Z-AlPMts and $C_{0.4}$-AlPMt. Although the adsorption capacities of IOMts toward phosphate increased in the order: $C_{0.4}$-AlPMt < $C_{1.0}$-AlPMt < $Z_{1.0}$-AlPMt < $Z_{0.4}$-AlPMt (Fig. 7a), the enhancement of adsorption capacities toward phosphate were increased in the order: $C_{1.0}$-AlPMt < $C_{0.4}$-AlPMt < $Z_{1.0}$-AlPMt ≈ $Z_{0.4}$-AlPMt (Fig. 5a),

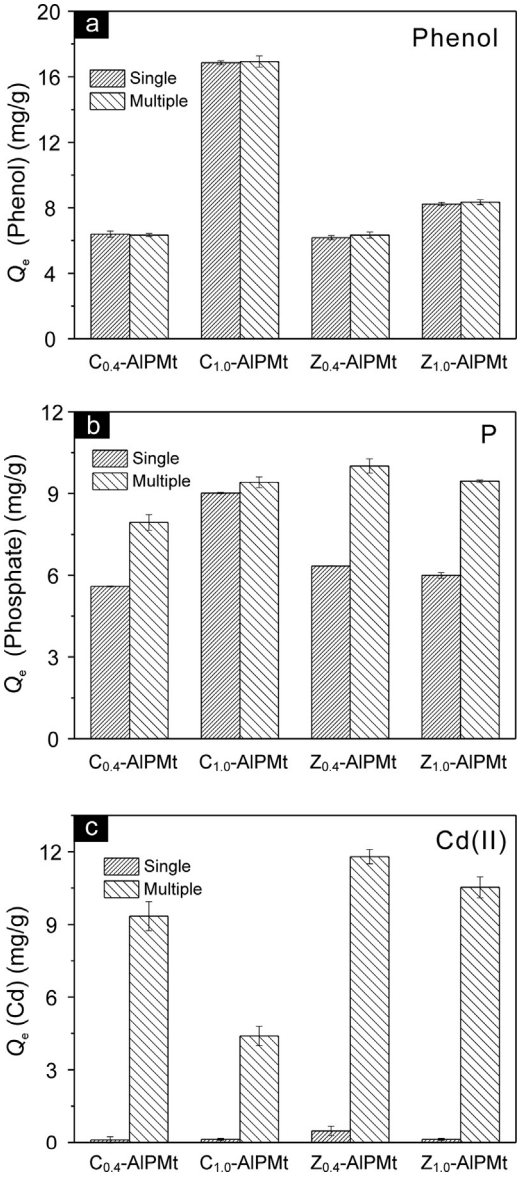

Fig. 5. Comparative adsorption of phenol (a), phosphate (b), and Cd(II) (c) on IOMts in single and multi-contaminant adsorption system ($C_{0,Phenol}$ = 200 mg/L, $C_{0,P}$ = 80 mg/L, C_{0Cd} = 90 mg/L).

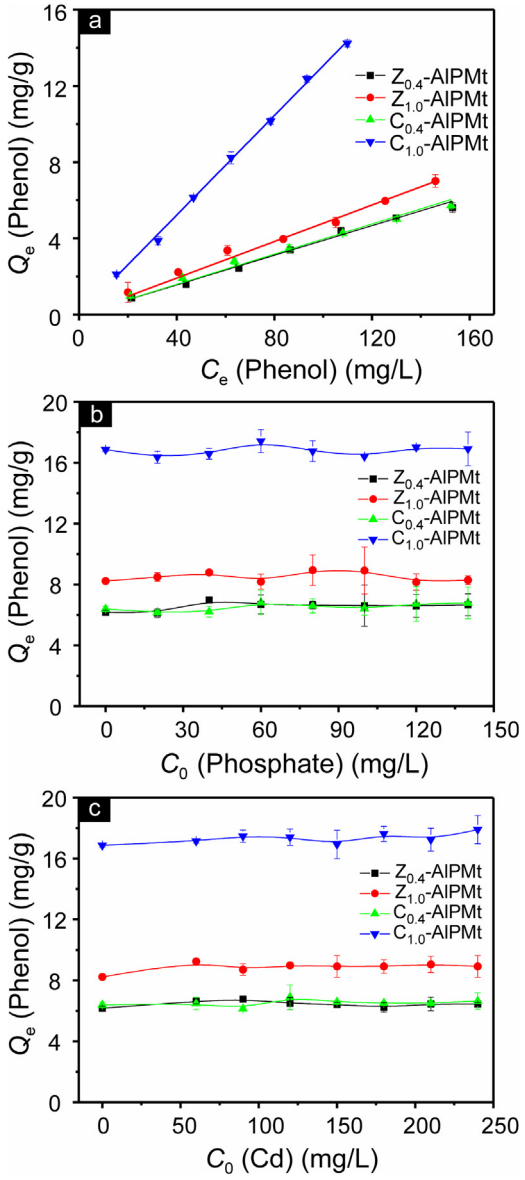

Fig. 6. Multi-contaminant adsorption results of phenol on IOMts: (a) adsorption isotherms of phenol on IOMts ($C_{0,P}$ = 80 mg/L, C_{0Cd} = 90 mg/L); (b) the effect of initial concentration of phosphate on the adsorption capacities of phenol on IOMts ($C_{0,Phenol}$ = 200 mg/L, C_{0Cd} = 90 mg/L); (c) the effect of initial concentration of Cd(II) on the adsorption capacities of phenol on IOMts ($C_{0,Phenol}$ = 200 mg/L, $C_{0,P}$ = 80 mg/L).

which is consistent with the order of Al_{13} contents on IOMts. This finding suggests that the additional adsorption sites for phosphate provided by the adsorption of Cd(II) might mainly exist on the surface of Al_{13} cations on IOMts.

For the adsorption of Cd(II) on IOMts in the multi-contaminant system, the equilibrium adsorption data were in good agreement with the Langmuir isotherm (Table 4), indicating that the monolayer adsorption on surface with a finite number of identical sites was the possible adsorption model for Cd(II) uptake. Compared with single contaminant adsorption system, the Langmuir adsorption capacities of IOMt toward Cd(II) were significantly enhanced in multi-contaminant system (Table 4). The enhancement is strongly dependent on the initial concentration of phosphate (Fig. 8c), indicating that the adsorption of phosphate provided a lot of additional adsorption sites for Cd(II). Although the adsorption capacity of $C_{1.0}$-AlPMt toward phosphate was higher than that of $C_{0.4}$-AlPMt in the multi-contaminant system, the adsorption of Cd(II) on $C_{1.0}$-AlPMt was much lower than that on $C_{0.4}$-AlPMt (Fig. 8a). The adsorption capacities of IOMts toward Cd(II) increased in the order:

Table 4
Langmuir and Freundlich equation parameters for the adsorption of Cd(II) on IOMts in single and multi-contaminant adsorption systems.

	Langmuir model			Freundlich model		
	Q_m (mg/g)	K_L (L/mg)	R^2	K_F	n	R^2
$C_{0.4}$-AlPMt	0.45	0.045	0.563	0.08	2.85	0.228
$C_{1.0}$-AlPMt	0.43	0.013	0.633	0.01	1.17	0.628
$Z_{0.4}$-AlPMt	0.81	0.019	0.795	0.08	2.64	0.388
$Z_{1.0}$-AlPMt	0.50	0.051	0.659	0.21	5.32	0.343
$C_{0.4}$-AlPMt/m*	14.10	0.045	0.991	3.58	4.02	0.927
$C_{1.0}$-AlPMt/m	10.12	0.010	0.955	0.49	2.01	0.963
$Z_{0.4}$-AlPMt/m	15.27	0.096	0.998	6.10	5.73	0.963
$Z_{1.0}$-AlPMt/m	14.14	0.085	0.999	5.00	5.045	0.914

* The adsorption isotherms of phosphate on C-AlPMts and Z-AlPMts in the multi-contaminant adsorption system ($C_{0,Phenol}$ = 200 mg/L and $C_{0,P}$ = 80 mg/L) were denoted as C_n-AlPMt/m and Z_n-AlPMt/m, respectively. (n = the dose of surfactant).

Table 5
Adsorption capacities of clay mineral-based materials for the phenol, phosphate and Cd(II).

Adsorbents	Adsorption capacity (mg/g)*	pH	Concentration range (mg/L)	References
Phenol				
Z16-Mt	9.90	5	175	[25]
C16-Mt	13.76	5	175	[25]
Bentonite	1.712		25–500	[40]
Amphoteric modified soil	~1.98	7.0–7.6	500	[41]
HMBP-montmorillonite	19.76	6	141.2	[42]
CTAB-Al_{10}-Bentonite	7.78	5.5	100	[20]
$C_{0.4}$-AlPMt	6.33	5	200	This study
$C_{1.0}$-AlPMt	16.93	5	200	This study
$Z_{0.4}$-AlPMt	6.33	5	200	This study
$Z_{1.0}$-AlPMt	8.34	5	200	This study
*Phosphate**				
AlPMt-1.0	10.36	5	20–140	[16]
AlPMt-2.0	14.79	5	20–140	[16]
AlPMt-4.0	16.78	5	20–140	[16]
CTAB-Al_{10}-Bentonite	7.63	5.5		[20]
Al-Bent	12.7	3	25–60	[13]
Fe-Bent	11.2	3	25–60	[13]
Fe-Al-Bent	10.5	3	25–60	[13]
$C_{0.4}$-AlPMt	10.07	5	20–140	This study
$C_{1.0}$-AlPMt	12.13	5	20–140	This study
$Z_{0.4}$-AlPMt	13.04	5	20–140	This study
$Z_{1.0}$-AlPMt	12.36	5	20–140	This study
*Cd(II)**				
AlPMt-1.0	22.17	5	30–240	[16]
AlPMt-2.0	22.88	5	30–240	[16]
AlPMt-4.0	23.09	5	30–240	[16]
Al_{13}-PAAMts	18.30	6.5		[11]
Fe-Mont	25.7	5	20–200	[12]
$C_{0.4}$-AlPMt	14.10	5	30–210	This study
$C_{1.0}$-AlPMt	10.12	5	30–210	This study
$Z_{0.4}$-AlPMt	15.27	5	30–210	This study
$Z_{1.0}$-AlPMt	14.14	5	30–210	This study

* The phosphate and Cd(II) adsorption capacities are the Langmuir adsorption capacities.

$C_{1.0}$-AlPMt < $C_{0.4}$-AlPMt < $Z_{1.0}$-AlPMt < $Z_{0.4}$-AlPMt (Fig. 5c), consistent with the Al contents of IOMts. These observations also suggest that the additional adsorption sites provided by adsorbed phosphate mainly exist on the surface of Al_{13} cations on IOMts, and the phosphate adsorbed by anion exchange with Br^- on $C_{1.0}$-AlPMt cannot provide the additional adsorption sites for the adsorption of Cd(II). Similar to the adsorption of phosphate on Z-AlPMt, the adsorption capacity of Cd(II) on Z0.4-AlPMt was slight higher than that on $Z_{1.0}$-AlPMt, indicating that the intercalated Z16 may adversely affect the adsorption of phosphate and Cd(II) since their Al contents were comparable.

Compared with the adsorption of phosphate, the adsorption capacities of IOMts toward Cd(II) were more dependent on the initial concentrations of phosphate and Al contents of IOMts in the multi-contaminant adsorption system. In addition, the enhancements of adsorption of Cd(II) on IOMts were much larger than that of phosphate (Fig. 5b and c). These finding suggests that Cd(II) did not directly bind to the mineral surface but to the adsorbed phosphate that was bound directly to the surface of Al_{13} cations on IOMts in the multi-contaminant adsorption system.

The strong interaction among intercalated Al_{13} cations, adsorbed phosphate, and Cd(II) in the multi-contaminant system indicated that the formation of P-bridged ternary surface complex might be the possible mechanism for the synergistic adsorption of phosphate and Cd(II) on IOMts. This means that phosphate directly binds to Al-OH surface of interlayer Al_{13} cations through a ligand-exchange mechanism, bridging the Al_{13} cation surface and Cd(II) and forming a =Al-P-Cd ternary surface complex. Then, the bound Cd may further adsorb phosphate, forming a =Al-P-Cd-P complex. Zhu et al., [14] have reported a similar bonding mode for the promoted co-adsorption of phosphate and Cd(II) on hydroxyliron-montmorillonite complex. Li et al., [36] also reported the formation of ternary surface complexes for the adsorption of Zn with glyphosate on aluminum oxide.

Because the adsorption mechanism of ternary adsorption system might be affected by solution pH, physiochemical properties of adsorbent and adsorption densities of contaminants [14,36–39], the other possible adsorption models cannot be ruled out. The synergistic adsorption mechanism of phosphate and Cd(II) on IOMts needs to be further studied by spectroscopic method and quantum mechanical calculations [36,39].

Although some other clay mineral-based materials had been used to remove phenol, phosphate, and Cd(II) from water (Table 5), simultaneous adsorption behaviors of phenol, phosphate, and Cd(II) on them was seldom reported. Compared to these reported clay mineral-based adsorbents, IOMts as a low-cost adsorbent shows comparable adsorption capacities toward all three contaminants in multi-contaminant adsorption system. Therefore, IOMt could potentially be used as a novel adsorbent in the wastewater treatment.

4. Conclusions

The structure characteristics of IOMts prepared by cationic and zwitterionic surfactants modified AlPMt strongly depended on the types and doses of surfactants. More C16 could be loaded on AlPMt than Z16 when the dose increased, but the Al_{13} contents of C-AlPMts were less than that of Z-AlPMt and AlPMt. In the single adsorption system, all resulting IOMts could efficiently remove phenol and phosphate from water, but not Cd(II). The $C_{1.0}$-AlPMt showed the highest adsorption capacity toward phenol and phosphate. In the case of the multi-contaminant adsorption system, because of the different adsorption sites on IOMts, the adsorptions of phenol on IOMts were not affected by other two inorganic

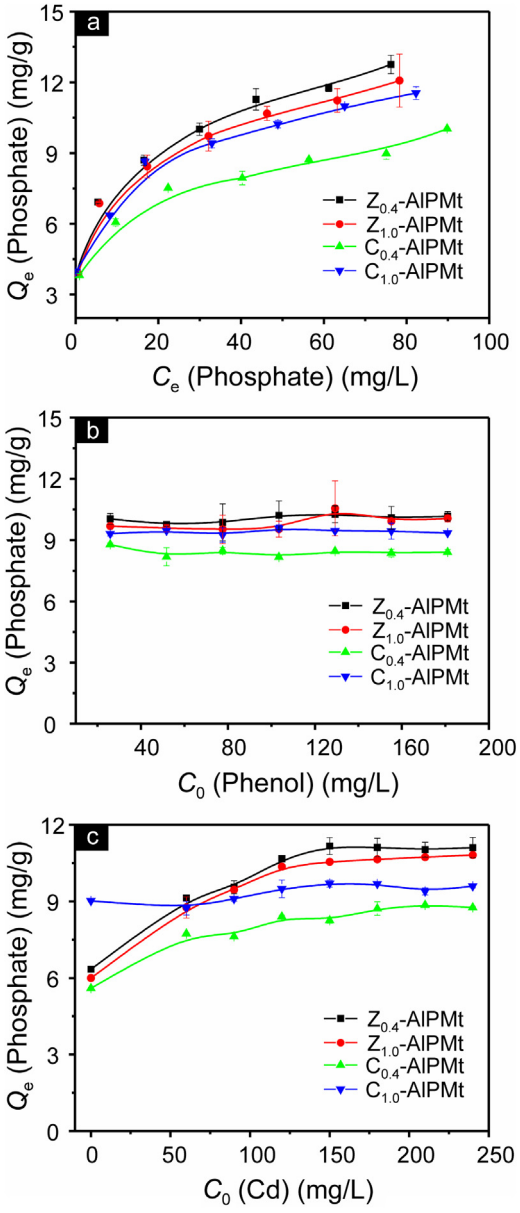

Fig. 7. Multi-contaminant adsorption results of phosphate on IOMts: (a) adsorption isotherms of phosphate on IOMts ($C_{0,Phenol}$ = 200 mg/L, C_{0Cd} = 90 mg/L); (b) the effect of initial concentration of phenol on the adsorption quantities of phosphate on IOMts ($C_{0,P}$ = 80 mg/L, C_{0Cd} = 90 mg/L); (c) the effect of initial concentration of Cd(II) on the adsorption quantities of phosphate on IOMts ($C_{0,P}$ = 80 mg/L, $C_{0,Phenol}$ = 200 mg/L).

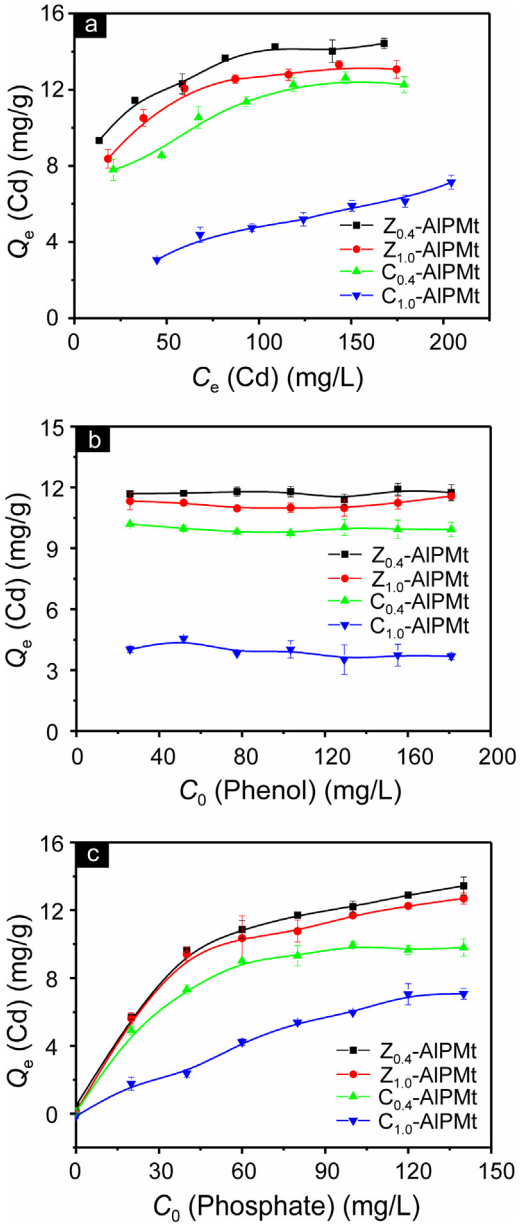

Fig. 8. Multi-contaminant adsorption results of Cd(II) on IOMts: (a) adsorption isotherms of Cd(II) on IOMts ($C_{0,P}$ = 80 mg/L, $C_{0,Phenol}$ = 200 mg/L); (b) the effect of initial concentration of phenol on the adsorption quantities of Cd(II) on IOMts ($C_{0,Cd}$ = 90 mg/L, $C_{0,P}$ = 80 mg/L); (c) the effect of initial concentration of phosphate on the adsorption quantities of Cd(II) on IOMts ($C_{0,Cd}$ = 90 mg/L, $C_{0,Phenol}$ = 200 mg/L).

components; neither did that of two inorganic components by phenol. The adsorptions of phosphate and Cd(II), however, were significantly enhanced in the multi-contaminant system, especially for the adsorption of Cd(II). The enhancements in adsorption of phosphate and Cd(II) were affected by the Al_{13} content of IOMts, indicated that the synergistic adsorption sites were mainly on the surface of Al_{13} content. The formation of phosphate-bridged ternary complex might be the possible adsorption mechanism for phosphate and Cd(II) on IOMts in the multi-contaminant system. Hence, the IOMts can efficiently remove NOCs, Cd(II) and phosphate from water in one step, and might be used as novel adsorbents to treat wastewater containing multi-contaminant.

Acknowledgements

We gratefully acknowledge the financial support from the National Natural Science Foundation of China (Grant No. 41272060, 41322014, 21177104, U1201233), the CAS-SAFEA International Partnership Program for Creative Research Team (Grant No. 20140491534), and Youth Innovation Promotion Association, CAS (Grant No. 2014324). We also thank the Queensland University of Technology's Vice Chancellor's research grant. This is contribution No. IS-2202 from GIGCAS.

References

[1] USEPA, TSCA work plan for chemical assessments: 2014 update, In: U.S. Environment Protection Agency (Ed.), 2014.

[2] D.L. Sparks, Toxic metals in the environment: the role of surfaces, Elements 1 (2005) 193–197.
[3] B. Pernet-Coudrier, W.X. Qi, H.J. Liu, B. Muller, M. Berg, Sources and pathways of nutrients in the semi-arid region of Beijing Tianjin, China, Environ. Sci. Technol. 46 (2012) 5294–5301.
[4] J.M. Salman, B.H. Hameed, Effect of preparation conditions of oil palm fronds activated carbon on adsorption of bentazon from aqueous solutions, J. Hazard. Mater. 175 (2010) 133–137.
[5] D. Mohan, K.P. Singh, Single- and multi-component adsorption of cadmium and zinc using activated carbon derived from bagasse—an agricultural waste, Water Res. 36 (2002) 2304–2318.
[6] E.W. Shin, J.S. Han, M. Jang, S.-H. Min, J.K. Park, R.M. Rowell, Phosphate adsorption on aluminum-impregnated mesoporous silicates: surface structure and behavior of adsorbents, Environ. Sci. Technol. 38 (2004) 912–917.
[7] F. Bergaya, G. Lagaly, Chapter 1—general introduction: clays, clay minerals, and clay science, in: F. Bergaya, G. Lagaly (Eds.), Developments in Clay Science, Elsevier, 2013, pp. 1–19.
[8] G.D. Yuan, B.K.G. Theng, G.J. Churchman, W.P. Gates, Chapter 5.1—clays and clay minerals for pollution control, in: F. Bergaya, G. Lagaly (Eds.), Developments in Clay Science, vol. 5B, Elsevier, 2013, pp. 587–644.
[9] B.L. Chen, W.H. Huang, J.F. Mao, S.F. Lv, Enhanced sorption of naphthalene and nitroaromatic compounds to bentonite by potassium and cetyltrimethylammonium cations, J. Hazard. Mater. 158 (2008) 116–123.
[10] B.K.G. Theng, G.J. Churchman, W.P. Gates, G. Yuan, Organically modified clays for pollutant uptake and environmental protection, in: Q. Huang, P. Huang, A. Violante (Eds.), Soil Mineral Microbe-Organic Interactions, Springer, Berlin Heidelberg, 2008, pp. 145–174.
[11] L.G. Yan, X.Q. Shan, B. Wen, G. Owens, Adsorption of cadmium onto Al13-pillared acid-activated montmorillonite, J. Hazard. Mater. 156 (2008) 499–508.
[12] P.X. Wu, W.M. Wu, S.Z. Li, N. Xing, N.W. Zhu, P. Li, J.H. Wu, C. Yang, Z. Dang, Removal of Cd2+ from aqueous solution by adsorption using Fe-montmorillonite, J. Hazard. Mater. 169 (2009) 824–830.
[13] L.G. Yan, Y.Y. Xu, H.Q. Yu, X.D. Xin, Q. Wei, B. Du, Adsorption of phosphate from aqueous solution by hydroxy-aluminum, hydroxy-iron and hydroxy-iron-aluminum pillared bentonites, J. Hazard. Mater. 179 (2010) 244–250.
[14] R.L. Zhu, M. Li, F. Ge, Y. Xu, J.X. Zhu, H.P. He, Co-sorption of cd and phosphate on the surface of a synthetic hydroxyiron-montmorillonite complex, Clays Clay Miner. 62 (2014) 79–88.
[15] M.X. Zhu, K.Y. Ding, S.H. Xu, X. Jiang, Adsorption of phosphate on hydroxyaluminum- and hydroxyiron-montmorillonite complexes, J. Hazard. Mater. 165 (2009) 645–651.
[16] L.Y. Ma, J.X. Zhu, Y.F. Xi, R.L. Zhu, H.P. He, X.L. Liang, G.A. Ayoko, Simultaneous adsorption of Cd(II) and phosphate on Al13 pillared montmorillonite, RSC Adv. 5 (2015) 77227–77234.
[17] R.L. Zhu, T. Wang, F. Ge, W.X. Chen, Z.M. You, Intercalation of both CTMAB and Al13 into montmorillonite, J. Colloid Interface Sci. 335 (2009) 77–83.
[18] L.Y. Ma, Q. Zhou, T. Li, Q. Tao, J.X. Zhu, P. Yuan, R.L. Zhu, H.P. He, Investigation of structure and thermal stability of surfactant-modified Al-pillared montmorillonite, J. Therm. Anal. Calorim. 115 (2014) 219–225.
[19] L.Y. Ma, J.X. Zhu, H.P. He, Q. Tao, R.L. Zhu, W. Shen, B.K.G. Theng, Al13 pillared montmorillonite modified by cationic and zwitterionic surfactants: a comparative study, Appl. Clay Sci. 101 (2014) 327–334.
[20] L.Z. Zhu, R.L. Zhu, Simultaneous sorption of organic compounds and phosphate to inorganic-organic bentonites from water, Sep. Purif. Technol. 54 (2007) 71–76.
[21] R.L. Zhu, L.Z. Zhu, J.X. Zhu, F. Ge, T. Wang, Sorption of naphthalene and phosphate to the CTMAB-Al13 intercalated bentonites, J. Hazard. Mater. 168 (2009) 1590–1594.
[22] C. Ouellet-Plamondon, R.J. Lynch, A. Al-Tabbaa, Comparison between granular pillared organo- and inorgano-organo-bentonites for hydrocarbon and metal ion adsorption, Appl. Clay Sci. 67–68 (2012) 91–98.
[23] S.Z. Li, P.X. Wu, Characterization of sodium dodecyl sulfate modified iron pillared montmorillonite and its application for the removal of aqueous Cu(II) and Co(II), J. Hazard. Mater. 173 (2010) 62–70.
[24] G.Y. Sheng, S.H. Xu, S.A. Boyd, A dual function organoclay sorbent for lead and chlorobenzene, Soil Sci. Soc. Am. J. 63 (1999) 73–78.
[25] L.Y. Ma, Q.Z. Chen, J.X. Zhu, Y.F. Xi, H.P. He, R.L. Zhu, Q. Tao, G.A. Ayoko, Adsorption of phenol and Cu(II) onto cationic and zwitterionic surfactant modified montmorillonite in single and binary systems, Chem. Eng. J. 283 (2016) 880–888.
[26] USEPA, Method 365.2, Methods for chemical analysis of water and wastes 2nd Ed, In: U.S. Environment Protection Agency (Ed.), Washington, DC, 1983.
[27] D. Plee, F. Borg, L. Gatineau, J.J. Fripiat, High-Resolution solid-State 27Al and 29Si nuclear magnetic-Resonance study of pillared clays, J. Am. Chem. Soc. 107 (1985) 2362–2369.
[28] L.Y. Ma, J.X. Zhu, H.P. He, Y.F. Xi, R.L. Zhu, Q. Tao, D. Liu, Thermal analysis evidence for the location of zwitterionic surfactant on clay minerals, Appl. Clay Sci. 112–113 (2015) 62–67.
[29] U.K. Saha, S. Hiradate, K. Inoue, Retention of phosphate by hydroxyaluminosilicate- and hydroxyaluminum-montmorillonite complexes, Soil. Sci. Soc. Am. J. 62 (1998) 922–929.
[30] T. Kasama, Y. Watanabe, H. Yamada, T. Murakami, Sorption of phosphates on Al-pillared smectites and mica at acidic to neutral pH, Appl. Clay Sci. 25 (2004) 167–177.
[31] A.A. Atia, Adsorption of chromate and molybdate by cetylpyridinium bentonite, Appl. Clay Sci. 41 (2008) 73–84.
[32] O. Maryuk, S. Pikus, E. Olszewska, M. Majdan, H. Skrzypek, E. Zieba, Benzyldimethyloctadecylammonium bentonite in chromates adsorption, Mater. Lett. 59 (2005) 2015–2017.
[33] K.Y. Foo, B.H. Hameed, Insights into the modeling of adsorption isotherm systems, Chem. Eng. J. 156 (2010) 2–10.
[34] D. Karamanis, P.A. Assimakopoulos, Efficiency of aluminum-pillared montmorillonite on the removal of cesium and copper from aqueous solutions, Water Res. 41 (2007) 1897–1906.
[35] E. Alvarez-Ayuso, A. Garcia-Sanchez, Removal of heavy metals from waste waters by natural and Na-exchanged bentonites, Clays Clay Miner. 51 (2003) 475–480.
[36] W. Li, Y.J. Wang, M.Q. Zhu, T.T. Fan, D.M. Zhou, B.L. Phillips, D.L. Sparks, Inhibition mechanisms of Zn precipitation on aluminum oxide by glyphosate: a 31P NMR and Zn EXAFS study, Environ. Sci. Technol. 47 (2013) 4211–4219.
[37] M. Grafe, M. Nachtegaal, D.L. Sparks, Formation of metal-arsenate precipitates at the goethite-water interface, Environ. Sci. Technol. 38 (2004) 6561–6570.
[38] P.J. Swedlund, J.G. Webster, G.M. Miskelly, Goethite adsorption of Cu(II), Pb(II), Cd(II), and Zn(II) in the presence of sulfate: properties of the ternary complex, Geochim. Cosmochim. Acta 73 (2009) 1548–1562.
[39] E.J. Elzinga, R. Kretzschmar, In situ ATR-FTIR spectroscopic analysis of the co-adsorption of orthophosphate and Cd(II) onto hematite, Geochim. Cosmochim. Acta 117 (2013) 53–64.
[40] F.A. Banat, B. Al-Bashir, S. Al-Asheh, O. Hayajneh, Adsorption of phenol by bentonite, Environ. Pollut. 107 (2000) 391–398.
[41] Z.F. Meng, Y.P. Zhang, Z.Q. Zhang, Simultaneous adsorption of phenol and cadmium on amphoteric modified soil, J. Hazard. Mater. 169 (2008) 292–498.
[42] Z.X. Luo, M.L. Gao, S.F. Yang, Q. Yang, Adsorption of phenols on reduced-charge montmorillonites modified by bispyridinium dibromides: mechanism, kinetics and thermodynamic studies, Colloid Surf. A 482 (2015) 222–230.